Neuron
Article

Temperature Entrainment of *Drosophila*'s Circadian Clock Involves the Gene *nocte* and Signaling from Peripheral Sensory Tissues to the Brain

Hana Sehadova,[1,5] Franz T. Glaser,[2,5] Carla Gentile,[1,5] Alekos Simoni,[1] Astrid Giesecke,[1,4] Joerg T. Albert,[3] and Ralf Stanewsky[1,2,*]
[1]School of Biological and Chemical Sciences, Queen Mary College, University of London, Mile End Road, London, E1 4NS, UK
[2]Institut für Zoologie, Universität Regensburg, Universitätsstrasse 31, 93040 Regensburg, Germany
[3]The Ear Institute, University College London, 332 Gray's Inn Road, London, WC1X 8EE, UK
[4]Present address: MRC Laboratory of Molecular Biology, Structural Biology Division, Hills Road, Cambridge CB2 0QH, UK
[5]These authors contributed equally to this work
*Correspondence: r.stanewsky@qmul.ac.uk
DOI 10.1016/j.neuron.2009.08.026

SUMMARY

Circadian clocks are synchronized by the natural day/night and temperature cycles. Our previous work demonstrated that synchronization by temperature is a tissue autonomous process, similar to synchronization by light. We show here that this is indeed the case, with the important exception of the brain. Using luciferase imaging we demonstrate that brain clock neurons depend on signals from peripheral tissues in order to be synchronized by temperature. Reducing the function of the gene *nocte* in chordotonal organs changes their structure and function and dramatically interferes with temperature synchronization of behavioral activity. Other mutants known to affect the function of these sensory organs also interfere with temperature synchronization, demonstrating the importance of *nocte* in this process and identifying the chordotonal organs as relevant sensory structures. Our work reveals surprising and important mechanistic differences between light- and temperature-synchronization and advances our understanding of how clock resetting is accomplished in nature.

INTRODUCTION

Circadian clocks regulate many biological processes so that they occur at beneficial times for the organism. Although these clocks are self-sustained and continue to run under constant conditions, they are synchronized with the environment by so called "Zeitgebers" (Dunlap et al., 2004). Two prominent Zeitgebers are the natural light-dark and temperature cycles that are able to synchronize the circadian clock of *Drosophila* and other organisms (see Boothroyd and Young, 2008; Dubruille and Emery, 2008; Glaser and Stanewsky, 2007 for recent reviews). Although our knowledge regarding light entrainment of both fly and mammalian clocks is quite advanced, relatively little is known about temperature synchronization. Light is generally considered to be the more powerful Zeitgeber, but a temperature cycle with only 2°C–3°C amplitude robustly synchronizes *Drosophila* behavioral rhythms (Wheeler et al., 1993). In mammals, chick, and zebrafish, similar low-amplitude temperature rhythms (equivalent to body-temperature rhythms) are able to synchronize clock gene expression in the suprachiasmatic nucleus (SCN) and peripheral clock cells (Barrett and Takahashi, 1995; Brown et al., 2002; Herzog and Huckfeldt, 2003; Kornmann et al., 2007; Lahiri et al., 2005; Prolo et al., 2005), exemplifying the potential strength of this Zeitgeber. Moreover, as shown for *Drosophila* (Glaser and Stanewsky, 2005), temperature synchronization of clock gene expression in these organisms occurs in tissue- or cell-autonomous manners, indicating that similar mechanisms are involved in ectothermic and endothermic animals.

Drosophila's daily locomotor rhythmicity profile is bimodal, exhibiting major activity peaks in the morning and evening (e.g., Wheeler et al., 1993). This bimodality is regulated by several groups of clock neurons in the fly brain (see Sheeba et al., 2008 for a recent review). Recent work has revealed that a group of ventrally located neurons controls mainly the morning activity peak of fly behavior (M-cells), whereas more dorsally located cells regulate evening activity (E-cells) (Sheeba et al., 2008). These neurons control locomotor rhythms, and cyclically express several clock genes and proteins in synchrony with light-dark or temperature cycles (e.g., Yoshii et al., 2005; Zerr et al., 1990).

While clock neurons are mainly cell autonomously synchronized by light via Cry, it is not known how temperature signals reach the brain clock. It is formally possible that temperature sensitive neurons express a circadian temperature receptor that is able to synchronize the molecular clock within the pacemaker neurons (Hamada et al., 2008). Alternatively, temperature could be sensed by other neurons in the brain or by sensory structures in other parts of the fly, which then signal to the clock neurons. Two mutations that interfere with temperature entrainment, both molecularly and behaviorally, have been identified and could therefore shed light on the temperature entrainment mechanism (Glaser and Stanewsky, 2005). Mutants in the *norpA*

gene, which encodes for the enzyme phospholipase C, are not able to synchronize to temperature cycles (Glaser and Stanewsky, 2005), indicating that a G protein-coupled signal transduction cascade might be involved. The mutated gene of the other temperature-entrainment-deficient variant (*nocte*) was not known until now.

Here we demonstrate that isolated *Drosophila* brains are not able to synchronize to temperature cycles. Since they do synchronize to light-dark cycles, these findings indicate that the brain requires temperature input from the periphery. We further reveal the molecular identity of the *nocte* gene, which encodes a large glutamine-rich protein with unknown function. Downregulation of *nocte* in peripheral tissues, including neurons of specific sensory structures (chordotonal [ch] organs), thoroughly disrupts temperature entrainment of behavioral rhythms. Similarly, other mutants known to affect the structure and function of ch organs also interfere with temperature entrainment, and mutant *nocte* alleles exhibit structural as well as physiological defects of sensory organ function. Moreover we show that a functional clock within these sensory structures is not required for behavioral temperature entrainment to occur, indicating that temperature information must be interpreted in a temporal fashion by downstream clock neurons in the thoracic central nervous system (CNS), or by the brain pacemaker neurons themselves. Our findings demonstrate the existence of a periphery-to-brain signaling pathway, identify the responsible sensory structures, and uncover fundamental differences between the light- and temperature-entrainment pathways of the fly circadian clock.

RESULTS

Tissue-Autonomous Synchronization to Temperature Cycles Is Restricted to Peripheral Organs

The *Drosophila* circadian clock can easily be entrained by temperature cycles (or steps), both in constant darkness (DD) and constant light (LL) (Busza et al., 2007; Glaser and Stanewsky, 2005; Matsumoto et al., 1998; Stanewsky et al., 1998; Wheeler et al., 1993; Yoshii et al., 2002, 2005, 2007). We previously showed that molecular synchronization can occur on a tissue-autonomous level. Isolated body parts of flies expressing two different *period-luciferase* (*per-luc*) constructs showed entrained bioluminescence oscillations when kept in LL and temperature cycles (Glaser and Stanewsky, 2005). When we performed these experiments, we noticed that isolated brains showed a 12 hr phase-advanced bioluminescence peak compared to all other isolated tissues (Figure 1A and Glaser and Stanewsky, 2005). This phase advance was not observed in LD cycles at constant temperature (Figure 1A), perhaps indicating a prominent role of the brain in synchronizing the phase of other tissues during temperature cycles. Alternatively, because the rise in *luc*-reported *per* expression occurs immediately after the temperature increase, it could reflect a mere response to the environmental transition, rather than bona fide synchronization of clock gene expression.

To address this issue we next analyzed brain *per-luc* expression in various mutant backgrounds known to interfere with temperature entrainment. We applied the *BG-luc* and *XLG-luc* transgenes, encoding 2/3 or the entire Per protein fused to Luc, respectively; both expressed under control of a 4.2-kb DNA fragment from the *per* promoter (Stanewsky et al., 1997; Veleri et al., 2003). Both the *norpA* and *nocte* mutations, previously shown to abolish molecular and behavioral synchronization by temperature (Glaser and Stanewsky, 2005), did not prevent the increase in brain *per-luc* expression after the temperature rise (Figure 1B). Next, we analyzed *per-luc* oscillations in the clock mutant backgrounds of tim^{01} and Clk^{Jrk} (Allada et al., 1998; Sehgal et al., 1994). Both mutations were previously shown to disrupt temperature entrainment at behavioral and molecular levels (Glaser and Stanewsky, 2005, 2007; Yoshii et al., 2002, 2005, 2007). Although temperature-induced oscillations were strongly suppressed in most clock mutant tissues analyzed, the brains again showed sharp increases of expression immediately after the change to the warm temperature (Figure 1B).

Because the rise in Luc activity occurred in clock-less mutant genetic backgrounds, the increase in reported *per* expression reflects a response to the temperature increase, rather than meaningful entrainment (which is read out as a cyclical phenomenon requiring an underlying oscillator). To address if this temperature-induced rise in Per-Luc expression occurs in clock neurons within the brain or in ectopic locations, we imaged brain bioluminescence signals using a highly sensitive imaging system (Figure 2). Brains were kept in cell culture medium in LL and temperature cycles and imaged at a time corresponding to the peak of *luc*-reported *per* expression (ZT8, Figures 1A and 1B). In a control experiment, brains were kept in LD cycles and constant temperature and imaged at ZT0, a time of high bioluminescence levels in brains (and other tissues) kept in LD (Figure 1A). In the LD control brains, luminescence signals could be detected in regions corresponding to various groups of clock neurons, presumably large and small Lateral Neurons ventral (LNvs), the dorsal Lateral Neurons (LNds), and two groups of the Dorsal Neurons (DNs) (Figure 2A, upper panel). Expression was also found in the ocelli and in the retina (Figure 2A, upper panel), previously shown to express *per* (Hall, 2003).

Surprisingly, brain expression in temperature cycles was not confined to cells that usually express clock genes. In a clock-normal genetic background, bioluminescence signals were restricted to the dorsal brain (Figure 2A). Compared to the LD expression pattern, the dorsal expression domain appeared broader, indicating that in addition to the DN located in this region, other cells now express the *XLG-luc* construct. Moreover, signals were clearly absent from brain regions where the lateral clock neurons are usually located. This cannot be explained by the constant presence of light (LL) (cf. Zerr et al., 1990), because Per is expressed in these clock neurons under LL and temperature cycling conditions in the intact animal (Yoshii et al., 2005). Strikingly, an almost identical expression pattern was observed in the tim^{01} genetic background, further indicating the non-clock-related nature of *luc*-reported *per* expression (Figure 2A). Similarly, in a Clk^{Jrk} mutant background, *BG-luc* expression occurred in a central brain region corresponding to the calyces of the mushroom bodies not known to contain any clock-gene-expressing cells (Figure 2A). Note that both *XLG-luc* and *BG-luc* transgenes are expressed in clock neurons

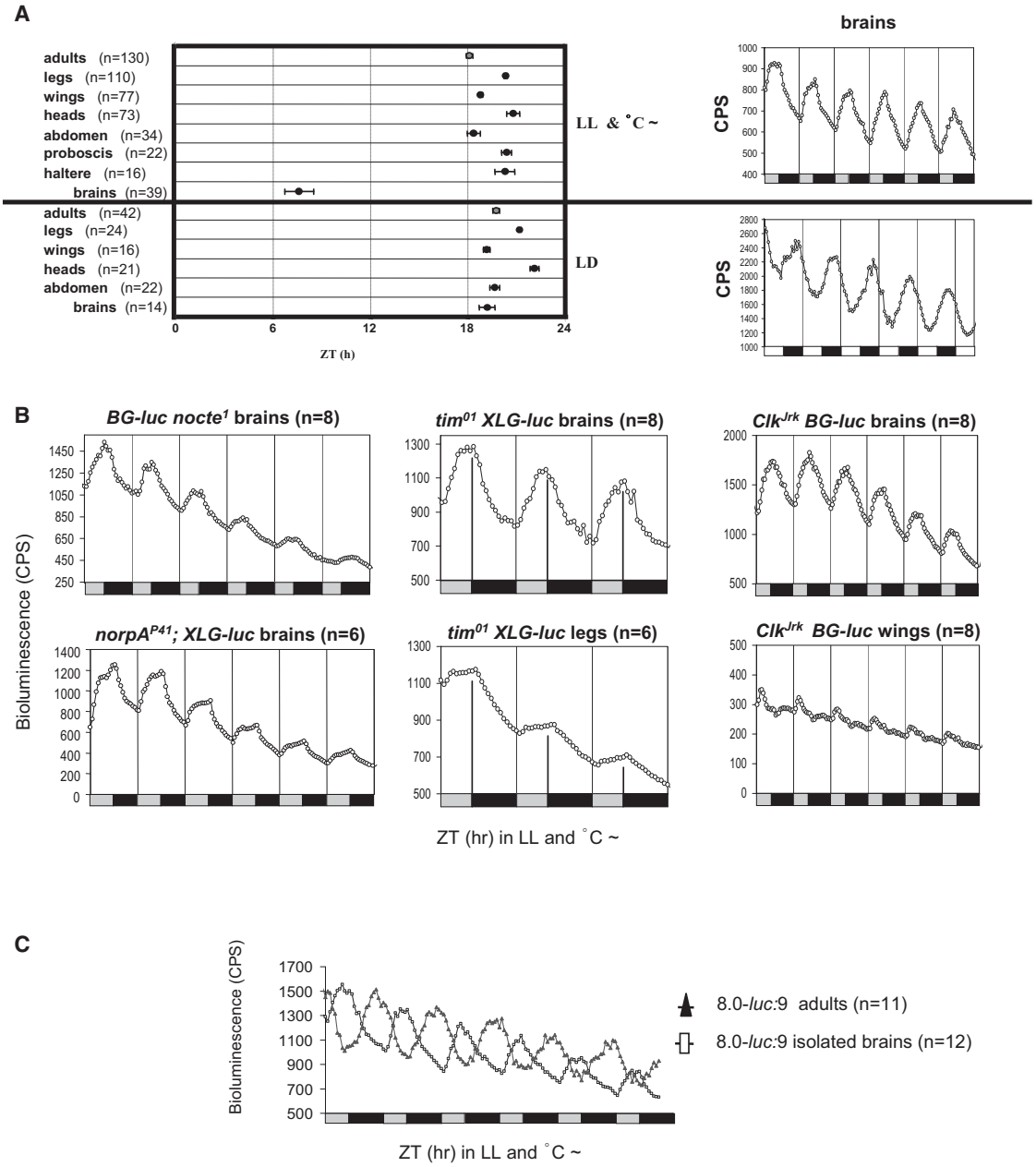

Figure 1. Cultured Brains Synchronize to Light-Dark, but Not to Temperature, Cycles

Isolated body parts or whole flies were either kept in light-dark cycles (LD) at 25°C or in constant light and 25°C:16°C temperature cycles (LL & °C~) as indicated in the figure.

(A) (Left) Phase comparison of bioluminescence peaks obtained from *XLG-luc* transgenic flies, in which the entire *period* (*per*) gene is fused to the *luciferase* (*luc*) cDNA. (Right) *XLG-luc* brains kept in LL & °C~ (top) or LD (bottom). Error bars indicate SEM. See Experimental Procedures for details about phase determination.

(B) Averaged bioluminescence recordings of different body parts from *XLG-luc* and *BG-luc* (containing a transgene encoding for two-thirds of the Per protein fused to *luc*) flies in different mutant backgrounds.

(C) Bioluminescence recordings from the *8.0-luc:9* transgenic type. This promoter-less *per-luc* construct encodes the entire Per protein and is predominantly expressed in dorsal clock neurons. White/gray and black bars indicate light/warm or dark/cold phase of the LD or temperature cycle, respectively.

during LD cycles (Stanewsky et al., 1997; Veleri et al., 2003; Figure 2A), indicating that the dramatic difference of spatial signal distribution between the two transgenic types observed in isolated brains during temperature cycling conditions depends more on the transgenic insertion site than on regulatory *per* sequences contained within the transgene. Importantly, in neither case does the spatial expression pattern significantly overlap with that of clock-gene-expressing cells under LD

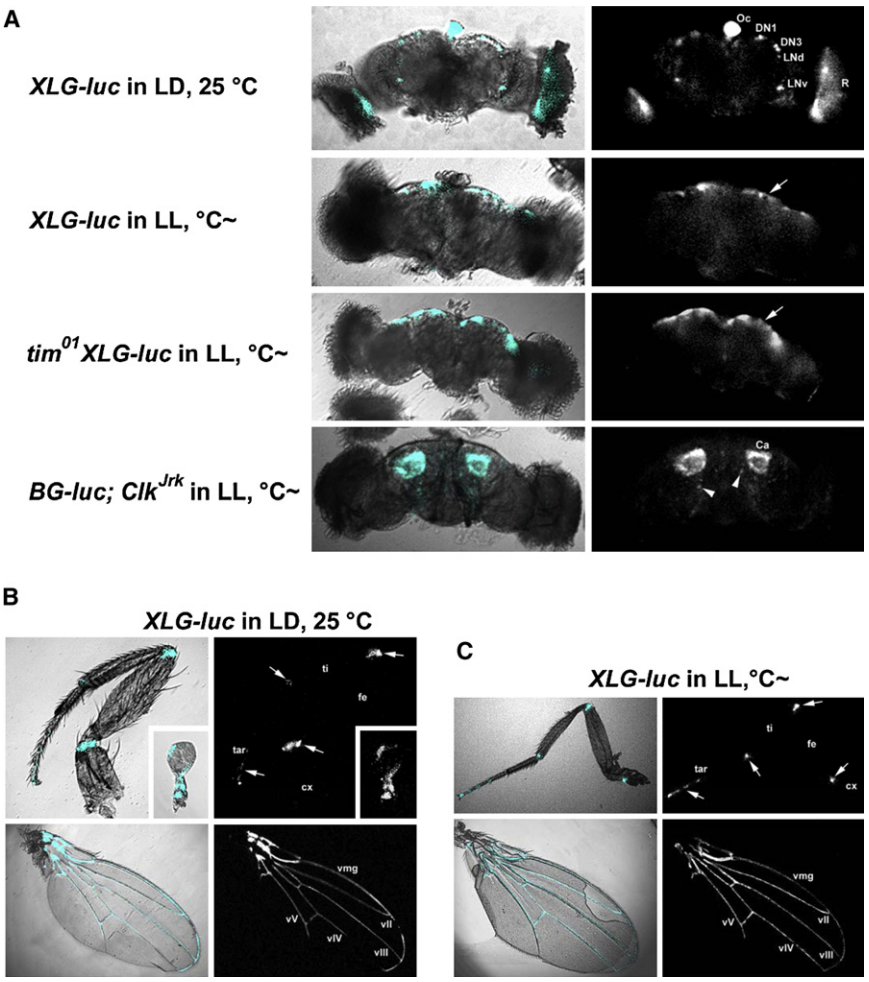

Figure 2. Spatial Per-Luc Expression in Brains Dramatically Differs after Light-Dark and Temperature Entrainment

(A) Brains dissected from *XLG-luc* flies and kept in LD at 25°C show bioluminescence signals in regions corresponding to the location of the clock neurons (DN1, DN3, LNd, LNv) and in the retina (R) and ocelli (Oc). In LL and temperature cycles (25°C:16°C), ectopic Per-Luc expression occurs in clock-normal and mutant genetic backgrounds (arrows) (see text for details). (B and C) Bioluminescence signals in peripheral tissues of *XLG-luc* flies kept in LD and 25°C or in LL and temperature cycles (25°C:16°C), respectively. Signals were detected in the joints of all leg segments, at the wing base, in ventral wing margin (vmg), in longitudinal wing veins (vII–vV), and in the scabellum, pedicel, and capitellum of the haltera (insets in B). cx, coxa; fe, femur; ti, tibia; tar, tarsus. (A–C) Left panels represent merged bioluminescence and bright-filed images; right panels show bioluminescence images.

conditions, pointing to a complete lack of spatial regulation of *per* under these conditions.

The ectopic Per-Luc expression observed in cultured brains—along with the lack of such signals from clock neurons—raised the possibility that spatial clock gene expression is generally altered in LL and temperature cycles compared to LD cycles at constant temperature. To test this, we imaged tissues known to synchronize under these conditions as well as in LD cycles (Glaser and Stanewsky, 2005; Figure 1A). Both legs and wings showed very similar spatial Per-Luc bioluminescence expression patterns under the two entrainment regimes, showing that peripheral clock tissues can be synchronized by light and temperature (Figure 2B).

In agreement with an earlier study describing *per-gal4*-driven GFP expression (Plautz et al., 1997), we also observe Per-Luc expression in potential mechanosensory and chemosensory cells along the wing margin and veins. In addition to what has been reported, we detected strong Per-Luc signals originating from the base of the wing, from the joints of the various leg segments (Figure 2B), and from segments of the haltere (inset in Figure 2B).

The *8.0-luc:9* line contains a promoterless *per-luc* fusion gene, which is expressed within a subpopulation of the DNs and occasionally in some LNd cells, but not in peripheral clock cells (Veleri et al., 2003). When *8.0-luc:9* adults were tested in LL and temperature cycles, bioluminescence peaks (presumably reflecting Per expression in brain clock neurons only) occurred late in the cold phase, similar as for the other Per-Luc transgenics tested (Figure 1C). When isolated brains were analyzed, we again observed a 12 hr phase shift, indicated by increased bioluminescence levels immediately following the temperature step up (Figure 1C).

Our results show that the brain has to be in the context of the intact fly in order for clock-neuronal gene expression to be synchronized by temperature cycles, and implies that in whole flies temperature entrainment involves signaling from peripheral tissues to the brain. As we will show below, this involves the gene *nocte*, a locus previously identified to play a role in temperature entrainment (Glaser and Stanewsky, 2005).

The *nocte* Gene Encodes a Large Glutamine-Rich Protein

In order to learn more about the function of *nocte* in temperature entrainment, we cloned the gene. Using meiotic mapping involving visible marker mutations and single nucleotide polymorphisms (SNPs), *nocte* was mapped to the 9A2–9D3 interval on the X chromosome (Experimental Procedures). Fine mapping using deficiencies placed *nocte* within the 9C1–9D2 interval containing 12 genes, flanked by the proximal breakpoint of $Df(1)c52,flw^{c52}$ (which removes 8E3-5;9C1; Tweedie et al., 2009) and the distal breakpoint of *Df(1)ED7010* (removing 9D3;9D4; Ryder et al., 2004) (Experimental Procedures). A chromosomal duplication covering this region ($Dp(1;2)v^{+75d}$ 9A2;10C2) rescued the

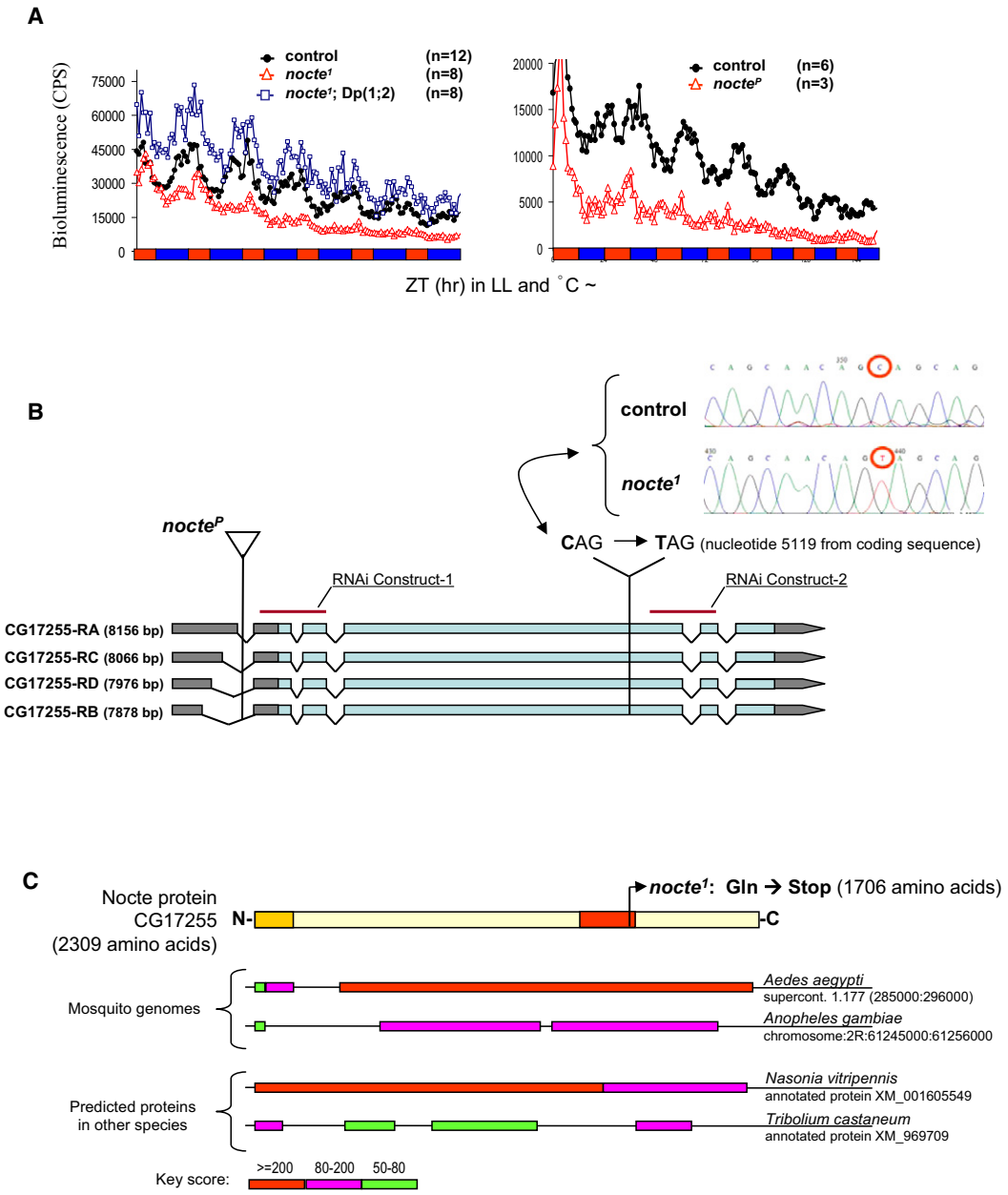

Figure 3. The *nocte* Gene Encodes a Large Glutamine-Rich Protein

(A) Bioluminescence recordings of *BG-luc* (left) and *XLG-luc* (right) adults in wild-type and *nocte* mutant flies. The *Dp(1;2)v*$^{+75d}$ (Dp(1;2)) covers the X chromosomal region 9A2–10C2 and rescues the phenotype of the EMS-induced *nocte*^{1} mutant.

(B) *nocte* gene structure, mRNA transcripts (gray: noncoding regions, blue: coding regions), location of the two mutant alleles, and the target regions of two *nocte* RNAi constructs (brown bars). In addition to the two transcript types reported in flybase (*CG17255-RA* and *RB*), we identified two additional transcripts by RT-PCR (*RC* and *RD*). All transcripts encode the same predicted protein and differ only in regard to the 5′-UTR (see also Figure S2).

(C) The predicted *Drosophila* Nocte protein has weak homology to the mammalian GRP-1 protein (red) and to the BAT2 domain of MHCIII genes (orange). *nocte*^{1} results in a truncated protein as indicated. In addition to other Drosophilidae, potential Nocte homologs were found in the mosquitoes *Aedes aegytpi* and *Anopheles gambiae* (Diptera), in the wasp *Nasonia vitripennis* (Hymenoptera), and in the beetle *Tribolium castaneum* (Coleoptera) (see Experimental Procedures for details).

molecular temperature entrainment defects of the original *nocte* mutant (Figure 3A), which confirmed the results of our mapping experiments. Next, we analyzed available mutations for the 12 candidate genes (Tweedie et al., 2009). One *P* element insertion line exhibited a temperature entrainment phenotype comparable to that observed in the original *nocte* mutant (Figures 3A, 4B, and 4C): wild-type flies anticipate the transition to the cold phase by an increase of their activity levels, which usually peak

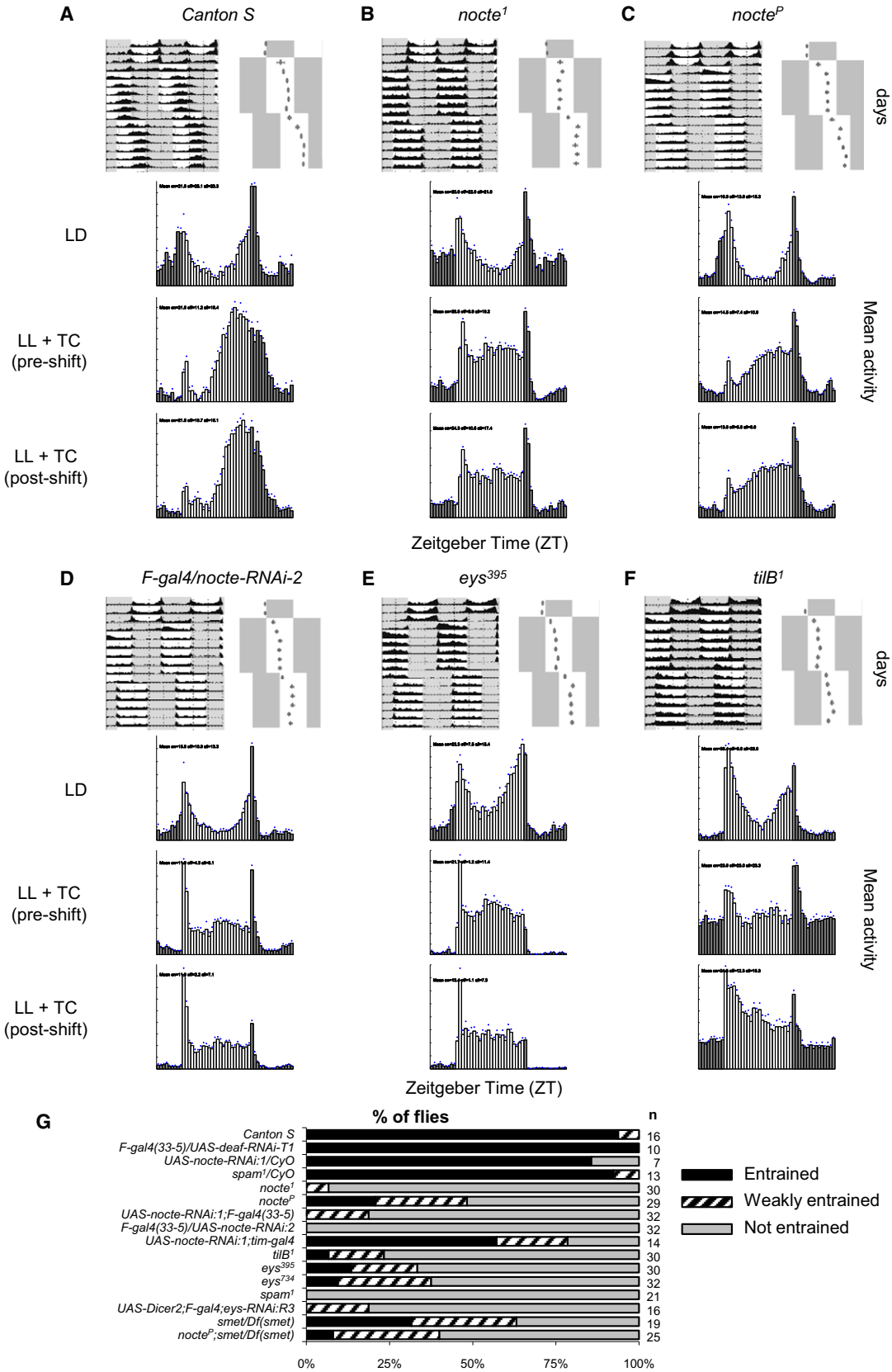
A
Canton S
B
nocte1
C
nocteP
days
LD
LL + TC
(pre-shift)
LL + TC
(post-shift)
Mean activity
Zeitgeber Time (ZT)
D
F-gal4/nocte-RNAi-2
E
eys395
F
tilB1
days
LD
LL + TC
(pre-shift)
LL + TC
(post-shift)
Mean activity
Zeitgeber Time (ZT)
G
% of flies
n
Canton S 16
F-gal4(33-5)/UAS-deaf-RNAi-T1 10
UAS-nocte-RNAi:1/CyO 7
spam1/CyO 13
nocte1 30
nocteP 29
UAS-nocte-RNAi:1;F-gal4(33-5) 32
F-gal4(33-5)/UAS-nocte-RNAi:2 32
UAS-nocte-RNAi:1;tim-gal4 14
tilB1 30
eys395 30
eys734 32
spam1 21
UAS-Dicer2;F-gal4;eys-RNAi:R3 16
smet/Df(smet) 19
nocteP;smet/Df(smet) 25
0%
25%
50%
75%
100%
Entrained
Weakly entrained
Not entrained

several hours before the actual transition (Busza et al., 2007; Glaser and Stanewsky, 2005), while flies carrying the chemically induced *nocte* allele do not show this anticipation, and simply react to temperature changes (Figure 4B) (Glaser and Stanewsky, 2005). Similarly, 80% of the flies carrying the insertion *P{lacW}CG17255*^{d07154}, or females heterozygous for the insertion and the original *nocte* allele, do not synchronize properly to temperature cycles, though they do entrain to LD (Figures 4C, 4G, and S1 available online). The insertion associated with this line is located in the first intron of the gene *CG17255* (Tweedie et al., 2009) (Figures 3B and S2) and results in the generation of abnormally spliced *CG17255* transcripts (Figure S2). We sequenced the open reading frame (ORF) of this gene in the original *nocte* mutant and in the background strain used to induce the original mutation (Experimental Procedures) and found that this mutant contains a single base pair change at nucleotide 5119 of the *CG17255* cDNA. This alteration introduces a premature stop codon (CAG → TAG) at position 1707 of the predicted protein, which normally is 2309 amino acids long (Figure 3C). Both mutations interfere with molecular and behavioral temperature entrainment, fail to complement each other, and affect the same transcription unit (Figures 3A, B, 4B, 4C, and S1). We therefore conclude that disruption of *CG17255* causes the observed phenotypes and named this gene *nocte*. The original ethyl methanesulfonate (EMS)-induced allele will from now on be referred to as *nocte*^{1}; the *P* element insertion as *nocte*^{P}. The *nocte*^{1} mutation maps to a portion of the gene's ORF that encodes one of several poly-glutamine stretches of Nocte. Apart from this feature and several poly-alanine stretches, Nocte has no apparent homologies to any other protein in the databases, except for a small region of similarity to the mammalian BAT2 domain at its N terminus (the overall similarity to the 70 N-terminal residues is weak, but it includes 11 identical amino acids). The BAT2 protein is encoded by a gene belonging the MHCIII class genes, but its function is unknown (Banerji et al., 1990). Nocte does not contain any cysteine residues, suggesting that it is an intracellular protein. Although Nocte has no apparent DNA binding domain, the presence of poly-Q and poly-A stretches also suggests that Nocte may function as transcription cofactor (Riley and Orr, 2006), which is further supported by a stretch of 268 amino acids showing weak homology to the mammalian Glutamine Rich Protein 1 (GRP-1) (Figure 3C; Cox et al., 1996). Comparison with available genome sequences revealed that *nocte* is distributed among insects (i.e., not only Drosophilidae; Figure 3C), but no obvious vertebrate homolog was identified (Experimental Procedures).

Downregulation of *nocte* in Peripheral Cells Interferes with Temperature Synchronization

Based on our finding that isolated peripheral tissues robustly synchronize to temperature cycles, but isolated brains do not (Figures 1 and 2), we wondered if *nocte* function in peripheral tissues may be required for temperature entrainment of the whole animal. For this, we generated two *nocte UAS-RNAi* transgenes (1 and 2) (Figure 3B, Experimental Procedures), and combined them (separately) with several *gal4*-containing transgenes that drive expression in various regions of the peripheral nervous system (PNS). Both *UAS-nocteRNAi* lines result in substantial downregulation of *nocte* mRNA in third-instar larvae, when crossed to *tim-gal4* or *nocte-gal4* (see below) driver lines, reducing mRNA levels to 20%–35% of peak levels (Figure S3). Synchronization to temperature cycles was analyzed by monitoring locomotor activity first in a 12 hr: 12 hr LD cycle at constant 25°C, followed by exposure to an out-of-phase 12 hr: 12 hr temperature cycle in LL for 1 week (previous light phase corresponded to the cryophase [16°C] and previous dark phase to the warm temperature [25°C]). This was followed by another such cycle, in which the onset of the warm phase was delayed by 6 hr compared to the initial temperature cycling regime (Figure 4). In this regime wild-type flies require 2–3 days to synchronize to the first temperature cycle and about the same number of days to resynchronize to the shifted temperature cycle. These "transients" are especially obvious when the activity peak phase plot (next to the actograms) is inspected (see Experimental Procedures and Figure S4 for how these plots were generated and how the ability to synchronize was determined and classified). In the daily average plots below the actograms, wild-type entrained behavior is characterized by a robust and defined activity peak in the second half of the warm phase, reflecting an anticipation of the transition to cold temperature (Figure 4A; Glaser and Stanewsky, 2005). Strikingly, the *F-gal4* transgenic (two independent insertion lines; Experimental Procedures), which is predominantly expressed in the neurons of the ch organs (Kim et al., 2003; Figures 5J–5R), produced a severe temperature entrainment defect (Figures 4D and 4G) when used to drive *nocte* RNAi-1 or 2. In the mutant plots the characteristic transients are missing or reduced and the animals largely react to the new temperature cycle. Apart from the reaction to the temperature change, the mutants remain rather constitutively active during the warm phase, not exhibiting the distinct anticipatory peak in the second half of the warm phase.

Interestingly, ~25% of the *nocte*^{P} mutant animals showed normal entrainment to temperature cycles, and another 25%

Figure 4. Downregulation of *nocte* in Peripheral Sensory Structures and Ch Organ Mutants Interferes with Behavioral Synchronization to Temperature Cycles

(A–F) Average actogram (left panels), activity peak phase (right panels), and daily activity plots (lower three panels) of flies that were entrained to 12 hr: 12 hr LD cycles for 3 days (LD) followed by 6 days of LL and 12 hr: 12 hr temperature cycles (25°C:16°C; LL + TC preshift) in which the warm and cold phase were in antiphase to the previous LD cycle. Subsequently, the onset of the warm phase was delayed by 6 hr compared to the initial regime (LL + TC postshift). Number of individual flies tested is indicated in (G). Note that all flies, except *Canton S* controls, show abnormal entrainment to temperature cycles but normal synchronization to LD. White bars or areas indicate light or warm phase and gray bars (areas) indicate dark or cold phase in LD and temperature entrainment conditions, respectively. Dots above the daily average bars indicate SEM. (G) Summary and quantification of behavior in temperature cycles for all genotypes tested. For *nocte-RNAi* lines *2:1b* and *1:3* are shown (Figure S3); for *tim-gal4* line, *16* was used. For classification criteria and methods see Experimental Procedures and Figure S4.

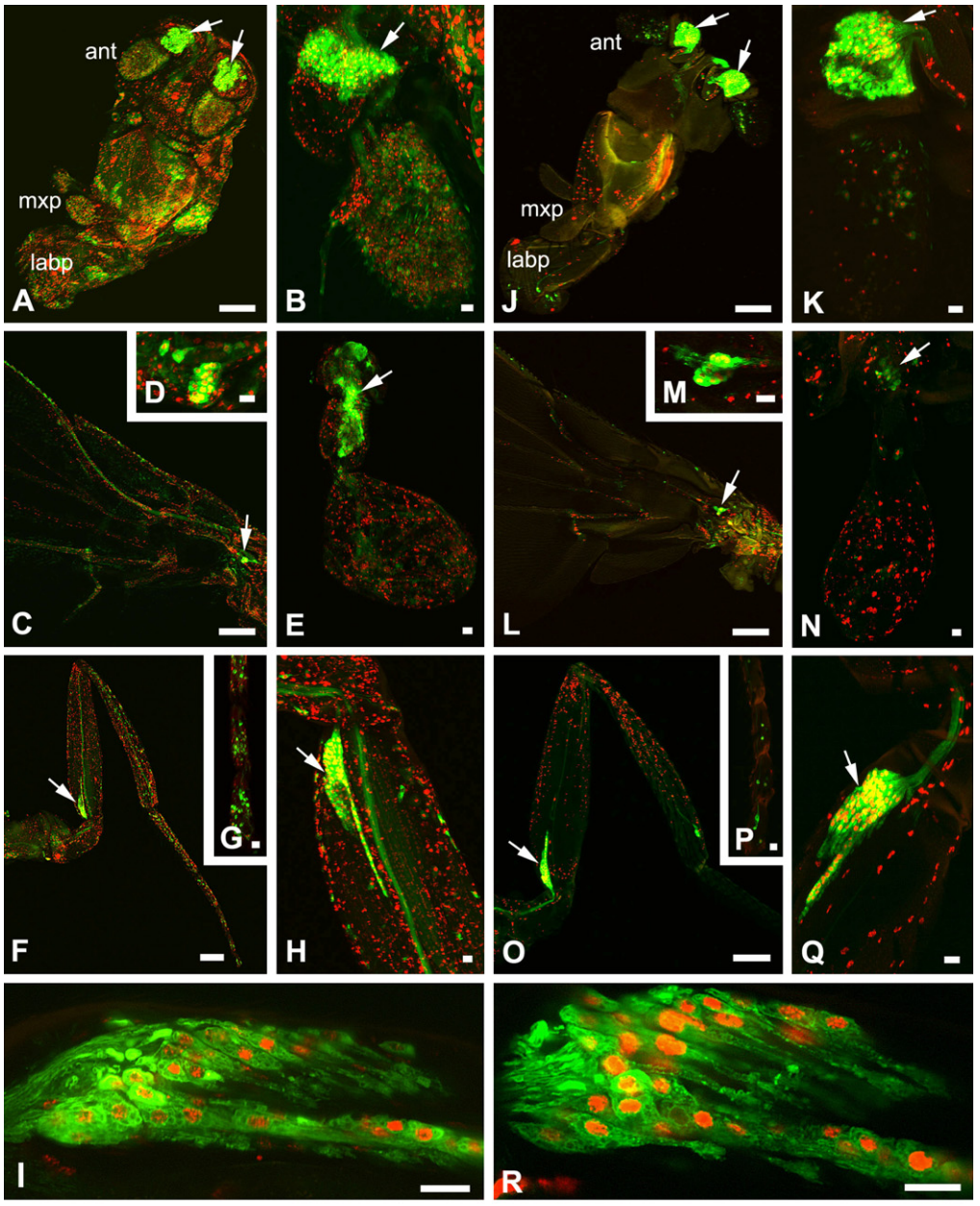
ant
mxp
labp
A
B
J
ant
mxp
labp
K
D
M
C
E
L
N
G
P
F
H
O
Q
I
R
S
nocte
+++
++
+
Relative RNA concentration
Head ♂
Head ♀
Brain ♂
Brain ♀
Ovary
Testis
Leg
Wing
T
nocte
Ext. body parts
ZT 4
ZT 16
Relative RNA concentration
ZT
period
ZT
Head ♂
Brain ♂
Leg ♀
Testis
Head ♀
Brain ♀
Wing ♀
Ovary

were weakly entrained (Figure 4G). This indicates that the *nocte*^{P} allele is a hypomorph, which is not surprising given that normally spliced *nocte* mRNAs can be detected in *nocte*^{P} flies (Figure S2).

As in *nocte* mutants, entrainment to LD cycles was not affected in *F-gal4/nocte-RNAi* flies, indicating a specific defect in temperature synchronization (Figures 4B–4D). Some *nocte* RNAi insertion lines (from both types) resulted in only mild temperature entrainment defects or even wild-type behavior (Figures S5A and S5D), indicating that positional effects of the transgene insertion site influence expression levels and RNAi efficiency (although levels of downregulation mediated by such "weak" RNAi lines were not assessed molecularly). These latter results, along with another control in which *F-gal4* was used to drive *deaf1*-RNAi (*deaf1* encodes a DNA binding protein unrelated to circadian clocks and ch organ function) (Veraksa et al., 2002; Figure 4G), also demonstrate that the temperature entrainment defects are not elicited by the *F-gal4* driver line alone.

F-gal4 Is Expressed in Ch and External Sense Organs

Adult ch organs are located at the joints between limb segments and are internally attached to the cuticle. They function as stretch receptors and the ch organs in adult legs and wings have been implicated in proprioception, whereas the one in antennae mediates hearing (Kernan, 2007). Neurons in larval body wall ch organs exhibit temperature-dependent calcium changes (Liu et al., 2003), but no connection between adult ch organs and temperature reception has been reported so far.

Careful analyses of *UAS-mCD8gfp* and *UAS-rfp* expression driven by the *F-gal4* transgene revealed that in addition to neurons of the ch organs (Figures 5Q and 5R), *F-gal4* is also expressed in a number of putative chemoreceptive and mechanoreceptive cells (external sense [es] organs) located in the labial and maxillary palpus (Figure 5J), first antennal segment (Figure 5K), wing (Figure 5L), haltere (Figure 5N), and leg (Figures 5O–5Q). Within the wing, *F-gal4*-positive cells were detected in the wing base, the ventral wing margin, and all wing veins, particularly in the regions close to the wing base. In the haltere and leg, *F-gal4*-positive cells are located in the cortex of every segment: marker signals were especially abundant in the capitellum of the haltere, the distal part of the femur, and the proximal part of the tibia. We also detected limited *F-gal4* expression in the brain (Figures S6 and S8).

Mutations Affecting the Ch Organs Show Deficits in Temperature Entrainment

To confirm the potential role of ch and es organs in temperature entrainment, we analyzed mutants affecting the *eyes shut* (*eys*) a.k.a. *spacemaker* (*spam*) gene that encodes a proteoglycan expressed in the interrhabdomeral space within the eye as well as within the luminal space of ch and es organs (Husain et al., 2006; Zelhof et al., 2006; Figure 6G). *eys* mutants lack the interrhabdomeral space, and as a consequence rhabdomeres are in close contact, leading to visual impairment, but no mechanosensory defects have been described (Husain et al., 2006). We tested three *eys/spam* alleles: *eys*^{734} and *eys*^{395} behave as loss-of-function mutants with respect to the rhabdomere phenotype, although Eys protein was detected in both mutants (Husain et al., 2006). The *spam*^{1} allele is protein null and exhibits the same rhabomere phenotype as the other two *eys* alleles (Zelhof et al., 2006). All three alleles showed wild-type behavior under LD conditions (Figure 4E and data not shown). Strikingly, in temperature cycles, 80% to 100% of the *eys/spam* mutant flies were mainly active during the warm phase, did not show the typical transients after transfer to a new temperature regime, and did not anticipate the temperature decrease, whereas the *spam*^{1} protein null allele showed the most severe phenotype (Figures 4E and 4G). The temperature synchronization defects observed for all three *eys/spam* alleles again indicate that ch and/or es organs are required for synchronization to temperature cycles and suggest that this function can be separated from their role in mechanoreception. Importantly, reducing *eys/spam* function in the ch and es organs using *F-gal4/eys-RNAi* also resulted in severely impaired behavioral synchronization to temperature in a manner similar to that as observed with *nocte-RNAi* (Figure 4G).

To specifically address the role of ch organs in temperature synchronization, we applied mutations of genes that are known to play a role in mechanoreception mediated by these organs and also retained normal es organ function. *touch insensitive larvaeB* (*tilB*) mutants have normal bristle receptor potentials but lack adult ch organ function, at least that of Johnston's organ (Eberl et al., 2000; Kernan, 2007). *tilB* encodes a protein conserved in ciliated eukaryotes that is required for ciliar structure and function (Kavlie, 2007; Tweedie et al., 2009). In *tilB*-mutant spermatids the axonemal structures of the cilia are disrupted, indicating that ciliary motility is impaired—the likely

Figure 5. Spatial and Temporal Expression Pattern of *nocte*

(A–R) Expression of *UAS-mCD8gfp* and *UAS-rfp* driven by *nocte-gal4* (A–I) and *F-gal4* (J–R) in potential chemoreceptors and mechanoreceptors and in neurons of the ch organs. (A and J) Signals in the labial (labp), maxillary palpus (mxp), antenna (ant), and antennal ch organs (arrows). (B and K) Larger magnification of the antenna. Arrow depicts neurons of the ch organ that project into the antennal nerve. (C and L) GFP and RFP signals in the wing base, ventral wing margin, all wing veins, and wing ch organ (arrow). (D and M) Wing ch organ. (E, F, N, and O) Signals in all segments of the haltere and leg. Arrows point to the ch organs. (G and P) Close-up of the last tarsal segments. (H, I, Q, and R) Leg ch organ (arrow). With *nocte-gal4*, both GFP and RFP signals were more abundant in all external organs tested. Intensity of GFP signals varied between "strong" in the ch organs and "weak" or "undetectable" in the chemoreceptors and mechanoreceptors, while RFP signals in all positive cells appear uniform. Scale bar for (A), (C), (F), (J), (L), and (O), 100 μm; for (B), (D), (E), (G–I), (K), (M), (N), and (P–R), 10 μm. (S) Comparison of the relative RNA expression of *nocte* in different body parts (normalized by *rp49*). ANOVA indicated highly significant differences of relative expression levels of *nocte* in the different body parts (ANOVA, $F_{7.88} = 55.11$; $p < 0.001$). According to LSD post hoc test ($p < 0.05$), they can be clustered in three groups of higher (+++), medium (++), and lower (+) *nocte* expression. (T) Temporal RNA expression of *nocte* (left panel) and *per* (right panel) in different body parts, under LL and temperature cycles (12 hr: 12hr, 25°C:16°C). Expression levels were normalized to *rp49*. Insets show the average of all body parts. Note that the apparent peak expression of *nocte* in the legs at ZT16 was not significant, nor could it be reproduced in an independent experiment in which mRNA levels in legs and wings were estimated at ZT4 and ZT16 (green histogram bars). Error bars in (S) and (T) indicate SEM. See Experimental Procedures for details.

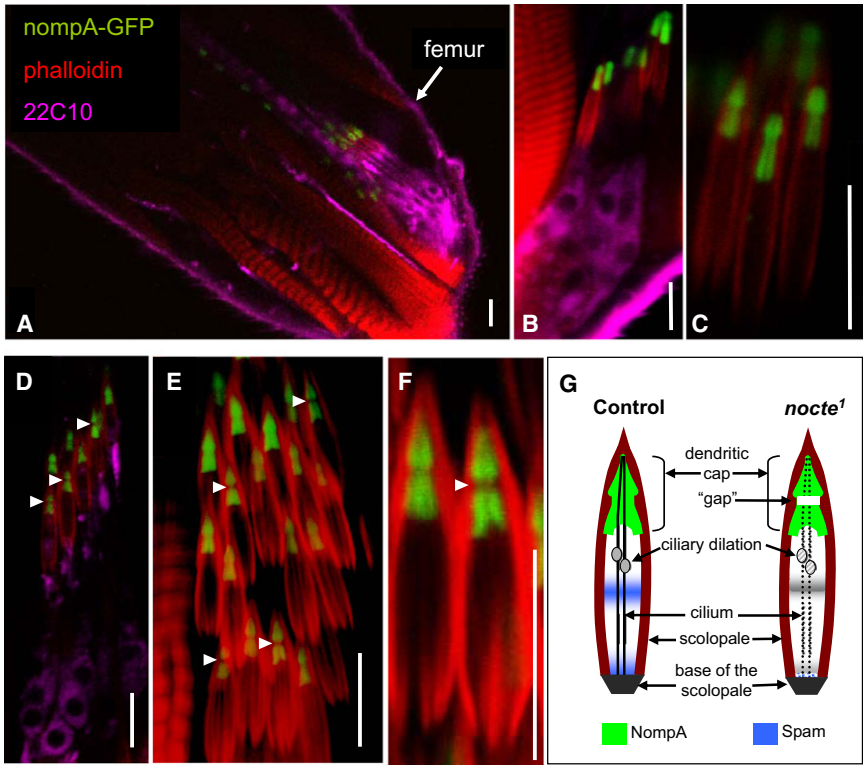

Figure 6. Altered Dendritic Caps or NompA Expression in the Femoral Ch Organs of *nocte*^{1} Flies

(A–C) Femur dissected from legs of *FM6* control and (D–F) *nocte*^{1} flies expressing the *gfp-nompA* construct. GFP-NompA (green) reports NompA expression in the dentritic cap of the scolopale. Cell bodies of ch organ neurons are visualized by 22C10 (magenta) and the scolopale actin capsule by phalloidin (red). Note that the ch organ neurons are the same as those expressing *F-gal4* and *nocte-gal4* in Figures 5I and 5R. Gaps detected in the NompA expression domain of *nocte*^{1} flies are indicated by arrow heads. Scale bars are 10 μm. (G) Cartoon showing structure and selected gene expression patterns in control and *nocte*^{1} mutant femoral scolopales (Kernan, 2007). Dotted structures indicate the uncertainty of the integrity of cilia, ciliary dilation (gray), and Spam/Eys distribution (blue) in *nocte*^{1}.

cause of sterility associated with this mutation (Caldwell et al., 2003). Although no such structural defect can be observed in adult ch organs at the light microscopy level, the same defect may underlie the deafness observed in *tilB* mutants (Kernan, 2007). *smetana* (*smet*) was isolated in a genetic screen for auditory mutants, and like *tilB*^{1}, causes male sterility and deafness, indicating a structural defect of the axoneme, but the mutated gene is not known (Caldwell et al., 2003). Strikingly, most *tilB*^{1} (90%) and *smet/Df(smet)* (65%) mutants show no or only weak synchronization to temperature cycles (Figures 4F and 4G). In order to determine potential genetic interactions between *nocte* and ch-organ-specific mutants, we generated a *nocte*^{P}*; smet/Df(smet)* double mutant. Interestingly, the double mutant flies exhibited a more sever temperature entrainment phenotype compared to the single mutants, indicating an additive effect and the involvement of both genes in the same process (Figure 4G). These results strongly implicate ch organs and the axonemal cytoskeleton surrounding the ch organ cilia as crucial components of the temperature input pathway.

nocte Is Expressed in Many Tissues, Including Ch and Es Organs

To determine if *nocte* is indeed expressed in the adult ch and es organs, we generated a *nocte-gal4* transgene by cloning an ~2 kb genomic DNA fragment upstream of the *nocte* transcription start into a *gal4* transformation vector (Experimental Procedures). Crossing several independently isolated *nocte-gal4* insertion lines to a reporter strain containing *UAS-mCD8gfp* and *UAS-rfp* transgenes revealed identical widespread, but not ubiquitous, activity of the *nocte* promoter fragment (Figures 5A–5I, S6, and S8). Positive tissues included those that can be synchronized by temperature cycles in isolation, but they also included the brain (Figures 5A–5I, S6, and S8). To validate the spatial expression pattern of *nocte*, we performed real-time PCR experiments on RNA isolated from different body parts, which confirmed the broad expression pattern observed with *nocte*-promoter-driven reporter expression (Figure 5S). Our expression data are also in good agreement with those reported in *FlyAtlas* for *CG17255* (Chintapalli et al., 2007). Quantitative RNA expression analysis revealed that *nocte* is neither circadianly nor temperature-dependently regulated in the tissues analyzed (Figure 5T, and data not shown).

Importantly, when we compared reporter signals in *F-gal4* and *nocte-gal4* flies, the ch and es organs of the adult legs, wings, haltere, and antennae were found to express *nocte* (Figures 5A–5R; Kim et al., 2003). In particular, strong neuronal expression in the ch organs was observed, similar to that reported for *F-gal4* (compare Figures 5I and 5R). Overall, the number of *nocte*-positive cells was larger than that obtained with the *F-gal4* driver, but they were located in the same regions (Figures 5A–5R). It therefore appears that the *F-gal4*-expressing cells are a subset of *nocte*-expressing ones. This is in good agreement with our finding that *nocte* function within *F-gal4*-expressing cells mediates temperature entrainment (Figure 4D).

Johnston's Organ Is Not Required for Temperature Entrainment

Because the antennal ch organ (Johnston's organ, located in the second antennal segment) of *Drosophila* is a highly specialized organ mediating hearing, we speculated that it is not required for temperature synchronization. On the other hand, a previous report (Sayeed and Benzer, 1996) revealed a receptor for temperature preference behavior to be located in the third antennal segment. We had already shown that the antennae

are not required for temperature-cycle-induced molecular clock gene oscillations (Glaser and Stanewsky, 2005). Here we tested flies, in which either the third antennal segments or the whole antennae (including Johnston's organ) were mechanically ablated, for their ability to synchronize behaviorally to LD and temperature cycles (Figures S5B and S5C). During both environmental cycles, behavior of the manipulated flies was very similar to that of wild-type, demonstrating that the antennae are not required for temperature entrainment. Although we cannot rule out a contribution of Johnston's organ, it seems clear that one or several of the other adult ch organs (Figures 5C–5I and 5L–5R) are sufficient for clock synchronization by temperature.

nocte Mutants Exhibit Visible Ch Organ Defects

Based on the involvement of *nocte* and ch organs in temperature entrainment, it was possible that *nocte* mutants affected ch organ structure. First we analyzed RFP expression in *F-gal4/nocte-RNAi/rfp* and *nocte^{1};F-gal4/rfp* flies and could not detect any gross structural abnormalities in the adult ch organ (Figure S7 and data not shown). In order to reveal potential alterations in the fine structure of ch organs, we crossed a *gfp-nompA* reporter gene into the genetic background of *nocte^{1}* and *nocte^{P}*. *gfp-nompA* encodes a GFP-NompA fusion protein, expressed under the control of the endogenous *nompA* promoter and recapitulating the spatial pattern of *nompA* expression (Chung et al., 2001). NompA is a transmembrane protein containing extracellular ZP domains, and is specifically expressed in the dendritic cap of ch and es organs (Figures 6A–6G; Chung et al., 2001). Inspection of GFP-NompA expression in femur ch organs revealed that between 60% (*nocte^{P}*) and 100% (*nocte^{1}*) of the *nocte* mutant flies tested contain dendritic caps that appear to have physical gaps, or spatially suppressed GFP-NompA expression (Figures 6D–6F and Table S1 available online). Since NompA is critical for transmission of mechanical stimuli from sensory structures to the sensory neuron (Chung et al., 2001), the structural defect, or the NompA expression phenotype we observed, indicates that ch organ function is also impaired in *nocte* mutants.

nocte Mutants Exhibit a Temperature-Dependent "Uncoordinated" Phenotype

The above results suggest that a structural defect in ch organs is responsible for the temperature synchronization defects observed in *nocte*, *tilB,* and *smet* mutants. Interestingly, one allele of the *eys/spam* locus (*spam^{1}*) also effects ch and es organ structure, but in a temperature- or humidity-dependent manner (Cook et al., 2008). It was shown that the Eys/Spam protein within the scolopale of ch organs conserves the shape and function of this structure after water loss induced by exposure to excessive heat or osmotic shock. In *spam^{1}* mutants this structural conservation is lost and the scolopales undergo dramatic cellular deformation, leading to flies that exhibit an irreversible uncoordinated locomotor phenotype after prolonged exposure to 37°C (Cook et al., 2008). Given that both *eys/spam* (including *spam^{1}*) and *nocte* mutants fail to entrain to temperature cycles (Figures 4B, 4C, 4E, and 4G), we wondered if *nocte* mutants also exhibit the same temperature-dependent uncoordinated phenotype. For this, we exposed control and nocte mutant flies

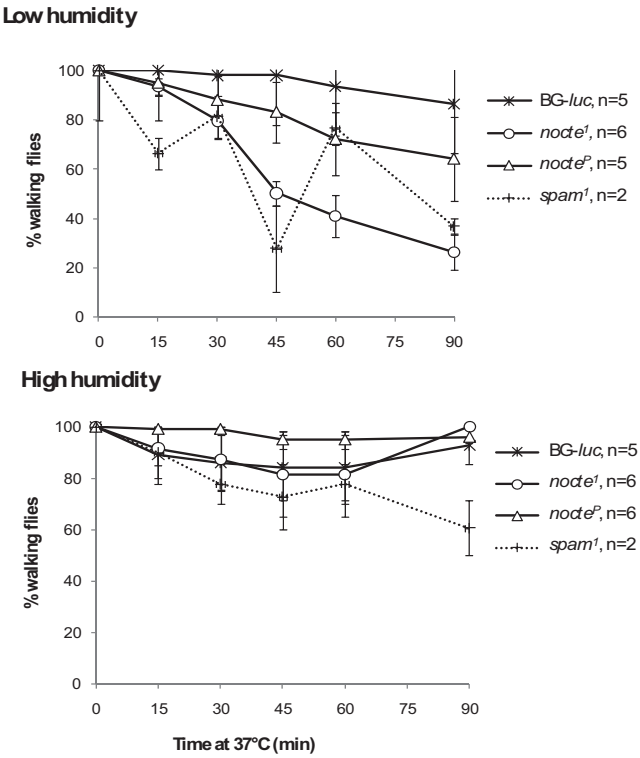

Figure 7. *nocte* Mutants Exhibit a Temperature-Dependent Uncoordinated Phenotype

Control (*BG-luc*), *nocte*, and *spam* mutant flies were raised at 25°C and transferred (in groups of 10) for 90 min to 37°C where they were observed every 15 min. The percentage of normal walking flies compared to "uncoordinated" flies is shown. The number of independent experiments (including 10 flies per genotype each) is indicated. Error bars indicate SEM.

to 37°C for 90 min and counted the number of flies that fell over during this time in 15 min intervals (Experimental Procedures; Cook et al., 2008). Both *nocte* alleles showed an uncoordinated phenotype, with more flies falling over the longer they were exposed to the high temperature (Figure 7). This phenotype was again more pronounced in *nocte^{1}* compared to *nocte^{P}*, further suggesting that the latter allele is a weak hypomorph. Interestingly, and as in the case of *spam^{1}* mutants, uncoordination was largely prevented when flies were exposed to the same high temperature at >90% humidity (Figure 7). This indicates that water loss from the scolopale also results in gross structural defects and cellular deformations of *nocte* ch organs, which may also explain why these organs fail to mediate temperature synchronization when mutated.

Temperature Entrainment Does Not Require a Functional Clock in the Ch Organs

We wanted to determine if a clock is required in the peripheral tissues expressing *F-gal4*. For this, we expressed a dominant-negative form of the *cycle* gene (*cycΔ*) in either all clock-gene expressing cells or the *F-gal4* pattern only. The *UAS-cycΔ* line causes arrhythmicity under DD and constant temperature

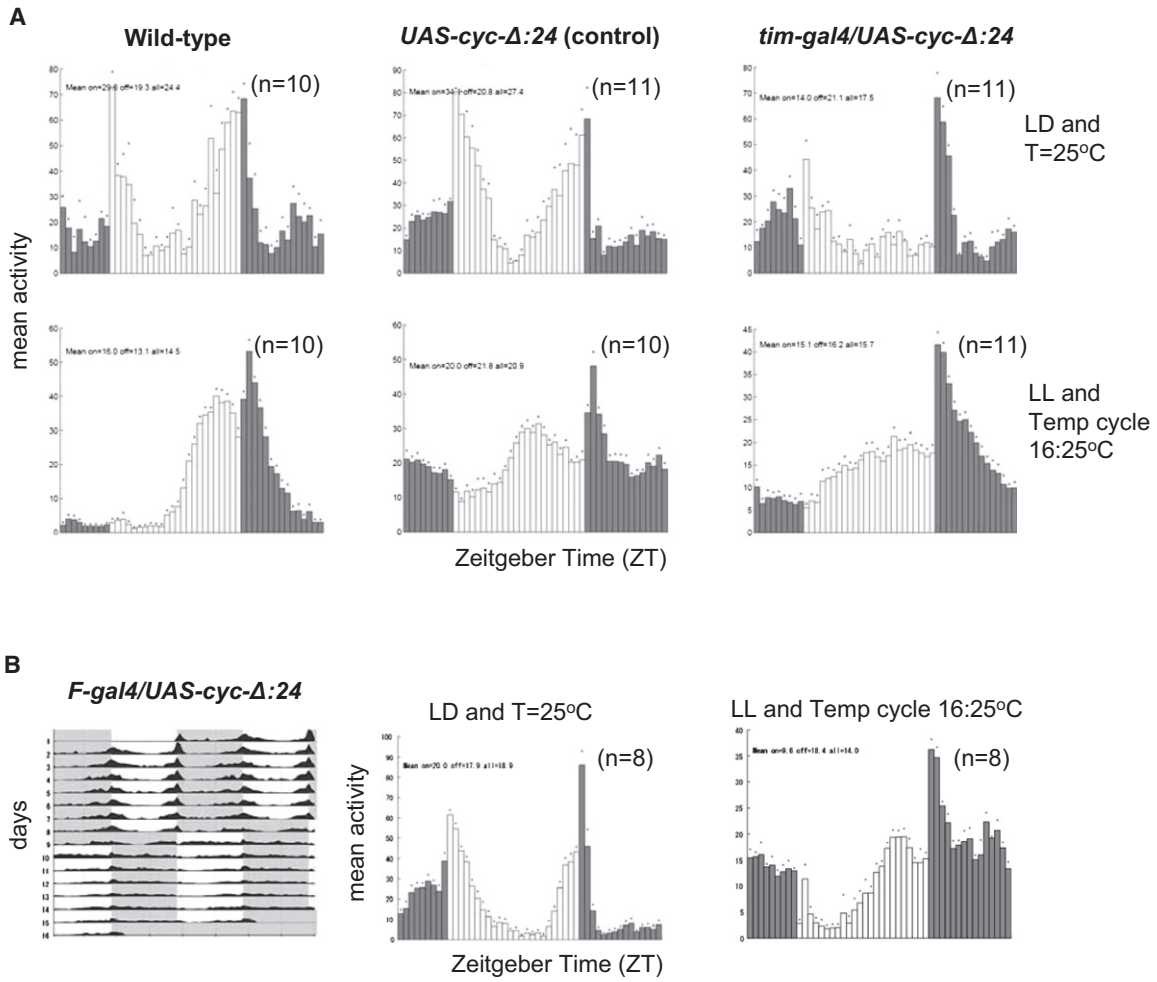

Figure 8. Peripheral Clocks in Ch Organs Are Not Required for Temperature Entrainment

Flies of the indicated genotypes were analyzed during 12 hr: 12 hr LD or temperature cycles, as indicated next to the panels.

(A) Expression of a dominant-negative form of the *cycle* gene (*cyc-Δ:24*) in all clock cells using the *tim-gal4* driver (line *27*). Wild-type (*Canton S*) and *UAS-cyc-Δ:24* flies were used as controls.

(B) *F-gal4/UAS-cyc-Δ:24* flies were entrained to LD for 3 days, followed by temperature cycles in LL, in which the warm and cold phase were in antiphase to the previous LD cycle. White and gray areas, bars, and SEM are as described in the legend to Figure 4.

conditions (Tanoue et al., 2004). As expected from the results obtained with the *tim* and *Clk* mutants (Figures 1B and 2A), *UAS-cycΔ* expression driven in all clock cells by the *tim-gal4* driver resulted in abnormal temperature entrainment (Figure 8A) (Yoshii et al., 2002, 2005). In contrast, when *UAS-cycΔ* was restricted to the *F-gal4*-expressing cells, temperature entrainment appeared normal (Figure 8B). This result is in good agreement with our failure to detect clock gene expression in ch organs (Figure S7), and also explains why *tim-gal4/UAS-nocteRNAi* flies entrain normally to temperature cycles (Figure 4G).

DISCUSSION

Temperature Entrainment of the Brain Clock Requires Signals from the Periphery

We show here unequivocally that isolated brains are not able to synchronize their circadian clock to temperature cycles, whereas they do entrain to LD. Tissue-autonomous synchronization to LD cycles is very likely mediated by the blue light photoreceptor Cry, which is expressed within a large subset of lateral and dorsal clock neurons (Benito et al., 2008; Yoshii et al., 2008). Likewise, synchronization of peripheral clock cells to light-dark and temperature cycles is tissue autonomous (Figure 1A). In contrast, brains depend on signals from the periphery for temperature entrainment to occur, indicating different temperature entrainment mechanisms for peripheral clock cells and central brain clock neurons. A possible reason for this may be that clock neurons need to be "protected" from imminent influences of temperature changes, which can occur very sporadically in nature. In fact, work from the Emery lab has shown that, even within the brain, a certain subset of light-responsive clock neurons that mainly controls the behavioral morning activity (M-cells) seems to repress temperature responsiveness of a different group of clock neurons (Busza et al., 2007).

Molecularly, this block could be mediated by Cry expression in the clock neurons, because it has been shown that the cry^b mutation enhances the amplitude of temperature-entrained clock gene expression (Glaser and Stanewsky, 2007). This suggests that some neurons are more responsive to a certain Zeitgeber than others and vice versa. For example, the Cry-negative neurons may be more important as temperature sensors as it was shown for the DN2 and Lateral Posterior Neurons (LPNs) located in the dorsal and lateral brain (Miyasako et al., 2007). These two neuronal groups do not (so far) belong to the M- and E-cell groups, and they can mediate aspects of temperature-entrained behavior in the absence of the M- and E-cells (Busza et al., 2007). In larvae the Cry-negative DN2 also play a prominent role under temperature entrainment conditions, where they seem to determine the phase of the other clock neurons in the larval brain (Picot et al., 2009).

It is conceivable that such a division of sensitivity to environmental signals, including complex protection from temperature signals in certain neurons, is required for stable synchronization to natural light-dark and temperature cycles. Since temperature cycles are a less reliable Zeitgeber compared to light-dark cycles, it would make sense that a peripheral temperature input is received only by a subset of clock neurons. These Cry-negative neurons are usually entrained by the light-responsive Cry-positive neurons, but under certain environmental conditions they could turn into the dominant neurons—now synchronizing the light-responsive neurons and activity rhythms to temperature cycles. The fact that temperature reception in these neurons occurs non-cell-autonomously (i.e., via the periphery) perhaps ensures that their input can more easily be controlled (i.e., shut off) by the clock-neuronal network.

Ch Organs as Circadian Temperature Receptors

We applied a set of PNS-*gal4* driver lines to home in on the tissues responsible for circadianly relevant temperature reception. This strategy was based on three observations: (1) PNS cells have been reported to express *per*, although a function for this expression is not known (Plautz et al., 1997); (2) isolated tissues containing these PNS cells are able to synchronize *per* expression to temperature cycles (Figures 1, 2, and Glaser and Stanewsky, 2005); and (3) *nocte* expression is also found within PNS cells of these tissues (Figure 5). We found that *F-gal4*, previously reported to be expressed specifically in ch organs, leads to disruption of temperature synchronization when crossed to *nocte-RNAi*. Although this immediately suggested that ch organs are crucial for this form of entrainment, careful inspection of the *F-gal4* expression pattern revealed that this driver is also active in es organs (Figure 5) and in a few neurons in the brain (Figures S6 and S8). Although *nocte* is also expressed in the brain, the spatial expression pattern of both genes appears to be distinct (Figures S6 and S8). Nevertheless, we cannot rule out that *nocte* and *F-gal4* are coexpressed in a few brain neurons and that *F-gal4*-mediated downregulation in brain neurons contributes to the observed temperature entrainment phenotype in *F-gal4/nocteRNAi* flies. In fact, *nocte*'s broad expression pattern in the brain does include the LNvs, and we could show that one LNv is also positive for *F-gal4* (Figure S8). But several observations strongly suggest that it is the prominent expression of *F-gal4* and *nocte* in ch organs that is mediating temperature entrainment. First, isolated brains do not synchronize to temperature cycles, indicating that *nocte* expression in the brain is not sufficient to mediate entrainment. Second, we found that mutations known to affect ch organ structure and function (*tilB*, *eys/spam*, *smet*) also interfere with temperature entrainment. Third, expression or function in the brain for any of these genes has not been described, and even if they do act in the brain it seems very unlikely that they are all expressed in the same putative "temperature entrainment cells." Fourth, if clock function is compromised in the one *F-gal4*-positive LNv via expression of the dominant-negative form of *cyc*, behavioral synchronization to temperature cycles is not affected (Figure 8B).

The *tilB* and *smet* mutants applied here are known to specifically affect ch function and leave es organ function intact (Caldwell et al., 2003; Eberl et al., 2000). Similarly, the $eys^{734/395}$ alleles retain normal mechanosensory function, but are thought to exhibit a molecular defect of the sensory dendrite of ch organs (Husain et al., 2006). All these mutations interfere with entrainment to temperature, but not to light-dark, cycles. Together with the prominent expression of *F-gal4* and *nocte* in ch organs, these findings strongly implicate ch organs as mediators of temperature entrainment, at least within the temperature interval applied in this study (25°C:16°C).

How May Ch Organs Perceive Temperature?

Ch organs can function as stretch receptors and have been implicated in mediating proprioception, gravireception, and vibration detection (Kernan, 2007). In contrast to external sensory cells, adult ch organs do not contain external bristles, and are attached to the inside of the cuticle. They consist of one to several hundred sensory units (scolopodia), and each of them contains a liquid-filled capsule (scolopale) that harbors the sensory endings of one to three neurons (Figure 6; Kernan, 2007). Interestingly, the Eys/Spam protein can be detected at the border between the ch neuron cell body and the lumen of the scolopale, and close to a characteristic dilation of the ch cilia (Cook et al., 2008; Husain et al., 2006). *spam* mutants exhibit a massive cellular deformation of the scolopale after exposure to 37°C (Cook et al., 2008). This deformation can be prevented by exposing the mutants to >90% humidity during the high temperature period. This suggests that the cellular deformation is caused by water loss from the hemolymph, which leads to water loss from the scolopale and subsequent neuronal deformation (Cook et al., 2008). *eys/spam* mutants show normal mechanoreceptor responses at room temperature, indicating that the presence of Eys/Spam protects the scolopale from excessive heat, probably by preventing water loss (Cook et al., 2008; Husain et al., 2006). *nocte* mutants exhibit the same temperature- and humidity-dependent uncoordinated phenotype as *spam* mutants, indicating a similar cellular deformation induced by excessive heat (Figure 7). Given that mutants of both genes also fail to synchronize to temperature cycles, we suspect that both phenotypes are related. As we show here, both *nocte* alleles lead to a structural defect in the dendritic cap of the ch organ (or misexpression of the dendritic cap protein NompA). It is conceivable that this defect also leads to excessive water loss at high temperatures, which would explain *nocte*'s

uncoordinated phenotype. For temperature entrainment to work properly it seems therefore absolutely crucial that the scolopale is protected from effects of extreme temperatures.

On the other hand, the ch organs must be able to sense subtle changes of temperature alterations in the fly's physiological range in order to function as circadian temperature sensors. In larvae, both ch organs and es neurons in the body wall react by increasing [Ca^{2+}] after raising or lowering the temperature (Liu et al., 2003), suggesting that they are also capable of detecting temperature changes in the adult. Considering that two other temperature entrainment mutants, *tilB* and *smet*, very likely affect the axonemal cytoskeleton structure of the ch cilia, we believe that perhaps dynamic properties of the ch cilia underlie temperature entrainment. The cilia in stimulated femoral ch organs of grasshoppers show active bending (i.e., not a passive reaction to the mechanical stimulus) close to the region where the cilia enters the scolopale (Moran et al., 1977). This ciliar bending presumably activates the ch neuron, which propagates the signal to the thoracic CNS. Interestingly, the same study showed that the femoral ch organ behaves tonically—in other words, it keeps firing at the same rate as long as the mechanical stimulation doesn't change (Moran et al., 1977). This inability to adapt to an environmental stimulus is exactly what would be required for a circadian temperature receptor, because it is necessary that it tracks subtle changes in temperature over time. Our current hypothesis therefore postulates the scolopale as an active unit for circadian temperature reception. Eys/Spam and Nocte are required to protect the unit from water loss at different temperatures, rendering the cilia able to react to subtle changes in temperature by actively changing its shape (perhaps by bending). The degree of ciliar bending then determines the firing frequency of the ch neuron, which is tightly coupled to the ambient temperature.

The Role of the *nocte* Gene Product in Temperature Entrainment

Both *nocte* alleles show similar phenotypes in regard to temperature entrainment, dendritic cap, and uncoordination phenotypes, although $nocte^{1}$ always exhibits more severe defects then $nocte^{P}$. This suggests that $nocte^{P}$ is a hypomorphic allele, a suggestion also supported by the observation that it is able to generate normally spliced transcripts in addition to aberrant ones (Figure S2). We also have evidence that $nocte^{1}$ is not a null allele, because (1) we can detect a truncated protein of the predicted size on western blots probed with an anti-Nocte serum, and (2) driving *nocte-RNAi* with broadly expressed *gal4* driver lines (e.g., *nocte-gal4, tim-gal4*) leads to adult lethality (C.G., H.S., A.S., A.G., and R.S., unpublished data).

Downregulation of *nocte* using *F-gal4* results in a severe temperature entrainment defect, confirming that this transcription unit is involved in the process. Because *F-gal4* is expressed within the neurons and cilia of ch organs, this behavioral defect indicates that *nocte* is also expressed in ch organ neurons (Kim et al., 2003). Based on the potential structural defect observed in *nocte* mutants, the Nocte protein may be required for the proper connection between the scolopale and the dendritic cap or proper expression and distribution of temperature-entrainment-relevant gene products along the cilia (Figure 6). This would also explain the structural defect or *nompA* misexpression phenotype caused by both *nocte* alleles (Figures 6D–6F and Table S1), which presumably underlies the observed temperature entrainment phenotype.

Requirement of a Functional Clock in Ch Organs

Our findings indicate that a functional clock within peripheral sensory structures important for temperature entrainment is not required (Figures 8 and S8). We therefore propose a model in which ch organ neurons, which do not possess a functional clock, send temperature information to peripheral clock neurons in the thoracic CNS, or directly to the more temperature-sensitive clock neurons within the brain (see above). A similar pathway has recently been described for sex peptide (SP) signaling, in which specific SP-receptor-expressing neurons located within the female reproductive tract signal to the CNS (Häsemeyer et al., 2009).

For daily temperature entrainment to work, temperature signals need to be interpreted by clock neurons in a time-dependent (i.e., circadian) manner in order to result in coordinated clock protein cycling and synchronized behavior controlled by these neurons. Neuronal brain clocks totally depend on these signals to become entrained by temperature, since they cannot synchronize in culture (Figures 1 and 2). Because isolated brains cell-autonomously synchronize to light (Figure 1), our findings reveal a fundamental difference between these two entrainment pathways.

EXPERIMENTAL PROCEDURES

Flies

For a detailed description of fly stocks used and generated for this study see Supplemental Experimental Procedures.

Bioluminescence Recordings and Imaging

Bioluminescence rhythms emanating from whole flies or individual body parts were recorded essentially as described (Glaser and Stanewsky, 2005) using an automated bioluminescence counter (Topcount, Perkin-Elmer). For more details, also regarding the generation of bioluminescence images shown in Figure 2 using the LuminoviewLV200 imaging system (Olympus, Tokyo, Japan), please refer to the Supplemental Experimental Procedures.

Mapping of *nocte*

By using visible markers, SNPs, chromosomal deficiencies, and insertions, *nocte* was mapped to the *CG17255* transcription unit at position 9C6–9D1 on the X chromosome. For details see Supplemental Experimental Procedures.

Generation of *nocte* Constructs

Nocte RNAi constructs were designed using fusions between *nocte* genomic and cDNA as described previously (Kalidas and Smith, 2002). For details see Supplemental Experimental Procedures.

Behavioral Analysis

Locomotor activity rhythms were recorded automatically using the *Drosophila* Activity Monitoring (DAM) system (Trikinetics, Waltham, MA) as previously described (Glaser and Stanewsky, 2005). Flies were initially synchronized and recorded in LD (12 hr: 12 hr) at a constant temperature of 25°C for 3–5 days and then released to LL and temperature cycles (12 hr: 12 hr, 25°C:16°C) in opposite phase to that of the initial LD cycle (i.e., cryophase corresponded to light, and warm phase to dark portion of the LD cycle). For the experiments shown in Figure 4, the temperature cycle was shifted after 6 days, so that the warm phase occurred in a 6 hr delay compared to the initial

temperature cycle, as indicated by the shading in the locomotor-activity plots (called actograms). For further details, please refer to the Supplemental Experimental Procedures.

Uncoordinated Assay and Quantification

The assay was performed as previously described (Cook et al., 2008). Flies were raised at 25°C and 10 young males were placed in a Petri dish and transferred for 90 min to a 37°C incubator where they were observed every 15 min. Relative humidity in the incubator was between 20%–30%. High humidity was obtained by adding a filter paper soaked in water to the Petri dish where the flies were monitored. The percentage of normal walking flies was determined by counting the number of flies walking at a certain time point and comparing it to the number of flies unable to walk or completely uncoordinated (i.e., lying on their backs or sides). High and low humidity observations were performed at the same time.

Fluorescence Microscopy and Immunohistochemistry

See Supplemental Experimental Procedures.

RNA Extractions and qPCR

Adult *Drosophila* (*y w*) were entrained for 3 days both under LD 25°C and LL 25°C:16°C (12 hr: 12 hr) conditions, and then collected at Zeitgeber Time (ZT) 0, 4, 8, 12, 16, and 20. Collection and dissection of 10 individuals started 30 min before and finished 30 min after each ZT. Wings, legs, and heads were immediately transferred to dry ice; brains, ovaries, and testis to RNA later solution (Ambion), and then stored at −80°C until RNA extraction. Two different *UAS-nocte-RNAi* transgenics (*nocte-RNAi2:1b* and *nocte-RNAi1:3*) were crossed with *tim-gal4:67* and *nocte-gal4:M3*. Crosses were kept at 18°C for 20 days and then transferred to 25°C. After four days at 25°C, five third-instar larvae were collected from each cross and from two of the parental lines (*nocte-RNAi1:3* and *tim-gal4:67*), and processed for quantitative PCR using a Reverse Transcription Reagents Kit (Applied Biossystems) (see Supplemental Experimental Procedures).

nocte Transcripts in *nocte*^{P} Mutants

Two samples of two adult female flies were collected in parallel from *Canton S* and *nocte*^{P} strains, and RNA extraction was performed as described above for samples used in qPCR and eluted in a final volume of 200 μl of H_2O. Reverse transcription reactions were performed with High Capacity RNA-to-cDNA Master Mix (Applied Biosystems) according to the manufacturer's instructions. PCR products from both strains were generated with *nocte*-specific primers and sequenced as described in the Supplemental Experimental Procedures.

Comparative Sequence Analysis to Identify *nocte* Homologs

Nocte protein sequence from *Drosophila melanogaster* was initially blasted (tblastn tool) against both the whole-genome shotgun reads on the NCBI website (http://blast.ncbi.nlm.nih.gov/Blast.cgi) and the available genomic sequences of insects on the Vector Base website (http://www.vectorbase.org/Tools/BLAST/). Several insect species were identified as potentially containing *nocte* homologs. In order to obtain a more specific blast result, the genomic regions with the best hits were downloaded and blasted (blastx tool) against the GeneBank protein sequences of *Drosophila melanogaster* in Flybase website (http://flybase.org/blast/). The most reliable candidates are presented in Figure 3C.

SUPPLEMENTAL DATA

Supplemental data for this article include eight Supplemental Figures, one Supplemental Table, and Supplemental Experimental Procedures and can be found at http://www.cell.com/neuron/supplemental/S0896-6273(09)00638-2.

ACKNOWLEDGMENTS

We thank OLYMPUS UK Ltd., namely Mr. Alan Kidger and Werner Kammerloher for their generous provision of the LuminoviewLV200, and Ko Fan Chen for help with *nocte* homology searches. We also thank C. Kim for the *F-gal4*; P. Hardin for *UAS-cyc Δ*, U. Tepass for *eys*; A. Zelhof for *spam*; D. Eberl for *tilB*, *smet*, and *gfp-nompA* flies; and P. Emery, J. Hall, and J. Levine for critical reading of the manuscript. Confocal imaging was performed with support of the Blizard Advanced Light Microscopy facility at Queen Mary. This work was supported by the Deutsche Forschungsgemeinschaft grants Sta 421/3-3 and Sta 421/6-6 given to R.S. Work in our lab is supported by EUCLOCK, an Integrated Project (FP6) funded by the European Commission and the BBSRC.

Accepted: August 19, 2009
Published: October 28, 2009

REFERENCES

Allada, R., White, N.E., So, W.V., Hall, J.C., and Rosbash, M. (1998). A mutant *Drosophila* homolog of mammalian Clock disrupts circadian rhythms and transcription of *period* and *timeless*. Cell *93*, 791–804.

Banerji, J., Sands, J., Strominger, J.L., and Spies, T. (1990). A gene pair from the human major histocompatibility complex encodes large proline-rich proteins with multiple repeated motifs and a single ubiquitin-like domain. Proc. Natl. Acad. Sci. USA *87*, 2374–2378.

Barrett, R.K., and Takahashi, J.S. (1995). Temperature compensation and temperature entrainment of the chick pineal cell circadian clock. J. Neurosci. *15*, 5681–5692.

Benito, J., Houl, J.H., Roman, G.W., and Hardin, P.E. (2008). The blue-light photoreceptor CRYPTOCHROME is expressed in a subset of circadian oscillator neurons in the *Drosophila* CNS. J. Biol. Rhythms *23*, 296–307.

Boothroyd, C.E., and Young, M.W. (2008). The in(put)s and out(put)s of the *Drosophila* circadian clock. Ann. N Y Acad. Sci. *1129*, 350–357.

Brown, S.A., Zumbrunn, G., Fleury-Olela, F., Preitner, N., and Schibler, U. (2002). Rhythms of mammalian body temperature can sustain peripheral circadian clocks. Curr. Biol. *12*, 1574–1583.

Busza, A., Murad, A., and Emery, P. (2007). Interactions between circadian neurons control temperature synchronization of *Drosophila* behavior. J. Neurosci. *27*, 10722–10733.

Caldwell, J.C., Miller, M.M., Wing, S., Soll, D.R., and Eberl, D.F. (2003). Dynamic analysis of larval locomotion in *Drosophila* chordotonal organ mutants. Proc. Natl. Acad. Sci. USA *100*, 16053–16058.

Chintapalli, V.R., Wang, J., and Dow, J.A. (2007). Using FlyAtlas to identify better *Drosophila melanogaster* models of human disease. Nat. Genet. *39*, 715–720.

Chung, Y.D., Zhu, J., Han, Y., and Kernan, M.J. (2001). *nompA* encodes a PNS-specific, ZP domain protein required to connect mechanosensory dendrites to sensory structures. Neuron *29*, 415–428.

Cook, B., Hardy, R.W., McConnaughey, W.B., and Zuker, C.S. (2008). Preserving cell shape under environmental stress. Nature *452*, 361–364.

Cox, G.W., Taylor, L.S., Willis, J.D., Melillo, G., White, R.L., 3rd, Anderson, S.K., and Lin, J.J. (1996). Molecular cloning and characterization of a novel mouse macrophage gene that encodes a nuclear protein comprising polyglutamine repeats and interspersing histidines. J. Biol. Chem. *271*, 25515–25523.

Dubruille, R., and Emery, P. (2008). A plastic clock: how circadian rhythms respond to environmental cues in *Drosophila*. Mol. Neurobiol. *38*, 129–145.

Dunlap, J.C., Loros, J.J., and DeCoursey, P.J. (2004). Chronobiolgy: Biological Timekeeping (Sunderland, Massachusetts: Sinauer Associates, Inc).

Eberl, D.F., Hardy, R.W., and Kernan, M.J. (2000). Genetically similar transduction mechanisms for touch and hearing in *Drosophila*. J. Neurosci. *20*, 5981–5988.

Glaser, F.T., and Stanewsky, R. (2005). Temperature synchronization of the *Drosophila* circadian clock. Curr. Biol. *15*, 1352–1363.

Glaser, F.T., and Stanewsky, R. (2007). Synchronization of the *Drosophila* circadian clock by temperature cycles. Cold Spring Harb. Symp. Quant. Biol. *72*, 233–242.

Hall, J.C. (2003). Genetics and molecular biology of rhythms in *Drosophila* and other insects. Adv. Genet. *48*, 1–280.

Hamada, F.N., Rosenzweig, M., Kang, K., Pulver, S.R., Ghezzi, A., Jegla, T.J., and Garrity, P.A. (2008). An internal thermal sensor controlling temperature preference in *Drosophila*. Nature *454*, 217–220.

Häsemeyer, M., Yapici, N., Heberlein, U., and Dickson, B.J. (2009). Sensory neurons in the *Drosophila* genital tract regulate female reproductive behavior. Neuron *61*, 511–518.

Herzog, E.D., and Huckfeldt, R.M. (2003). Circadian entrainment to temperature, but not light, in the isolated suprachiasmatic nucleus. J. Neurophysiol. *90*, 763–770.

Husain, N., Pellikka, M., Hong, H., Klimentova, T., Choe, K.M., Clandinin, T.R., and Tepass, U. (2006). The agrin/perlecan-related protein eyes shut is essential for epithelial lumen formation in the *Drosophila* retina. Dev. Cell *11*, 483–493.

Kalidas, S., and Smith, D.P. (2002). Novel genomic cDNA hybrids produce effective RNA interference in adult *Drosophila*. Neuron *33*, 177–184.

Kavlie, R.G. (2007). Touch insensitive larva B, a gene necessary for hearing and male fertility in *Drosophila melanogaster*, encodes a conserved ciliary protein. PhD thesis, University of Iowa, Iowa City, Iowa.

Kernan, M.J. (2007). Mechanotransduction and auditory transduction in *Drosophila*. Pflugers Arch. *454*, 703–720.

Kim, J., Chung, Y.D., Park, D.Y., Choi, S., Shin, D.W., Soh, H., Lee, H.W., Son, W., Yim, J., Park, C.S., et al. (2003). A TRPV family ion channel required for hearing in *Drosophila*. Nature *424*, 81–84.

Kornmann, B., Schaad, O., Bujard, H., Takahashi, J.S., and Schibler, U. (2007). System-driven and oscillator-dependent circadian transcription in mice with a conditionally active liver clock. PLoS Biol. *5*, e34.

Lahiri, K., Vallone, D., Gondi, S.B., Santoriello, C., Dickmeis, T., and Foulkes, N.S. (2005). Temperature regulates transcription in the zebrafish circadian clock. PLoS Biol. *3*, e351.

Liu, L., Yermolaieva, O., Johnson, W.A., Abboud, F.M., and Welsh, M.J. (2003). Identification and function of thermosensory neurons in *Drosophila* larvae. Nat. Neurosci. *6*, 267–273.

Matsumoto, A., Matsumoto, N., Harui, Y., Sakamoto, M., and Tomioka, K. (1998). Light and temperature cooperate to regulate the circadian locomotor rhythm of wild type and *period* mutants of *Drosophila melanogaster*. J. Insect Physiol. *44*, 587–596.

Miyasako, Y., Umezaki, Y., and Tomioka, K. (2007). Separate sets of cerebral clock neurons are responsible for light and temperature entrainment of *Drosophila* circadian locomotor rhythms. J. Biol. Rhythms *22*, 115–126.

Moran, D.T., Varela, F.J., and Rowley, J.C., 3rd. (1977). Evidence for active role of cilia in sensory transduction. Proc. Natl. Acad. Sci. USA *74*, 793–797.

Picot, M., Klarsfeld, A., Chelot, E., Malpel, S., and Rouyer, F. (2009). A role for blind DN2 clock neurons in temperature entrainment of the *Drosophila* larval brain. J. Neurosci. *29*, 8312–8320.

Plautz, J.D., Kaneko, M., Hall, J.C., and Kay, S.A. (1997). Independent photoreceptive circadian clocks throughout *Drosophila*. Science *278*, 1632–1635.

Prolo, L.M., Takahashi, J.S., and Herzog, E.D. (2005). Circadian rhythm generation and entrainment in astrocytes. J. Neurosci. *25*, 404–408.

Riley, B.E., and Orr, H.T. (2006). Polyglutamine neurodegenerative diseases and regulation of transcription: assembling the puzzle. Genes Dev. *20*, 2183–2192.

Ryder, E., Blows, F., Ashburner, M., Bautista-Llacer, R., Coulson, D., Drummond, J., Webster, J., Gubb, D., Gunton, N., Johnson, G., et al. (2004). The DrosDel collection: a set of *P*-element insertions for generating custom chromosomal aberrations in *Drosophila melanogaster*. Genetics *167*, 797–813.

Sayeed, O., and Benzer, S. (1996). Behavioral genetics of thermosensation and hygrosensation in *Drosophila*. Proc. Natl. Acad. Sci. USA *93*, 6079–6084.

Sehgal, A., Price, J.L., Man, B., and Young, M.W. (1994). Loss of circadian behavioral rhythms and *per* RNA oscillations in the *Drosophila* mutant *timeless*. Science *263*, 1603–1606.

Sheeba, V., Kaneko, M., Sharma, V.K., and Holmes, T.C. (2008). The *Drosophila* circadian pacemaker circuit: Pas De Deux or Tarantella? Crit. Rev. Biochem. Mol. Biol. *43*, 37–61.

Stanewsky, R., Jamison, C.F., Plautz, J.D., Kay, S.A., and Hall, J.C. (1997). Multiple circadian-regulated elements contribute to cycling *period* gene expression in *Drosophila*. EMBO J. *16*, 5006–5018.

Stanewsky, R., Kaneko, M., Emery, P., Beretta, B., Wager-Smith, K., Kay, S.A., Rosbash, M., and Hall, J.C. (1998). The cry^b mutation identifies *cryptochrome* as a circadian photoreceptor in *Drosophila*. Cell *95*, 681–692.

Tanoue, S., Krishnan, P., Krishnan, B., Dryer, S.E., and Hardin, P.E. (2004). Circadian clocks in antennal neurons are necessary and sufficient for olfaction rhythms in *Drosophila*. Curr. Biol. *14*, 638–649.

Tweedie, S., Ashburner, M., Falls, K., Leyland, P., McQuilton, P., Marygold, S., Millburn, G., Osumi-Sutherland, D., Schroeder, A., Seal, R., and Zhang, H. (2009). FlyBase: enhancing *Drosophila* Gene Ontology annotations. Nucleic Acids Res. *37*, D555–D559.

Veleri, S., Brandes, C., Helfrich-Forster, C., Hall, J.C., and Stanewsky, R. (2003). A self-sustaining, light-entrainable circadian oscillator in the *Drosophila* brain. Curr. Biol. *13*, 1758–1767.

Veraksa, A., Kennison, J., and McGinnis, W. (2002). DEAF-1 function is essential for the early embryonic development of *Drosophila*. Genesis *33*, 67–76.

Wheeler, D.A., Hamblen-Coyle, M.J., Dushay, M.S., and Hall, J.C. (1993). Behavior in light-dark cycles of *Drosophila* mutants that are arrhythmic, blind, or both. J. Biol. Rhythms *8*, 67–94.

Yoshii, T., Sakamoto, M., and Tomioka, K. (2002). A temperature-dependent timing mechanism is involved in the circadian system that drives locomotor rhythms in the fruit fly *Drosophila melanogaster*. Zoolog. Sci. *19*, 841–850.

Yoshii, T., Heshiki, Y., Ibuki-Ishibashi, T., Matsumoto, A., Tanimura, T., and Tomioka, K. (2005). Temperature cycles drive *Drosophila* circadian oscillation in constant light that otherwise induces behavioural arrhythmicity. Eur. J. Neurosci. *22*, 1176–1184.

Yoshii, T., Fujii, K., and Tomioka, K. (2007). Induction of *Drosophila* behavioral and molecular circadian rhythms by temperature steps in constant light. J. Biol. Rhythms *22*, 103–114.

Yoshii, T., Todo, T., Wülbeck, C., Stanewsky, R., and Helfrich-Förster, C. (2008). Cryptochrome is present in the compound eyes and a subset of *Drosophila*'s clock neurons. J. Comp. Neurol. *508*, 952–966.

Zelhof, A.C., Hardy, R.W., Becker, A., and Zuker, C.S. (2006). Transforming the architecture of compound eyes. Nature *443*, 696–699.

Zerr, D.M., Hall, J.C., Rosbash, M., and Siwicki, K.K. (1990). Circadian fluctuations of Period protein immunoreactivity in the CNS and the visual system of *Drosophila*. J. Neurosci. *10*, 2749–2762.